

PHYSICOCHEMICAL PROBLEMS
OF MATERIALS PROTECTION

Corrosion Protection Properties of 4-hydroxy-*N'*-[(1*E*, 2*E*)-3-phenylprop-2-en-1-ylidene] Benzohydrazide on Mild Steel in Hydrochloric Acid Medium¹

Preethi Kumari P^a, Prakash Shetty^b, and Suma A Rao^a

^aDepartment of Chemistry, Manipal Institute of Technology, Manipal University, Manipal, 576104 India

^bDepartment of Printing and Media Engineering, Manipal Institute of Technology, Manipal University, Manipal, 576104 India

e-mail: prakash.shetty@manipal.edu

Received August 6, 2014

Abstract—The corrosion behaviour of mild steel immersed in 0.5 M HCl in the absence and presence of 4-hydroxy-*N'*-[(1*E*, 2*E*)-3-phenylprop-2-en-1-ylidene] benzohydrazide (HPB) was evaluated using Tafel polarization and electrochemical impedance spectroscopy techniques. The effect of inhibitor concentration and temperature on the corrosion inhibition efficiency (% *IE*) of HPB was studied and discussed. It is observed that the inhibition efficiency increased with increase in inhibitor concentration and also with increase in temperature for a give inhibitor concentration. The polarization study revealed that HPB acts as a mixed type of inhibitor by inhibiting both anodic and cathodic reactions. The corrosion inhibition process follows Langmuir-adsorption isotherm and takes place predominantly through chemisorption.

DOI: 10.1134/S2070205115060143

1. INTRODUCTION

Mild steel is extensively used in industrial manufacturing, particularly in the automotive and machinery segments, due to its low production costs coupled with excellent mechanical properties, moderately high strength to weight ratio and overall integral reliability [1]. Acidic solutions are extensively used in acid cleaning, pickling, for the removal of rust and scale formed during forming processes. Steel surfaces deployed in service in such environments undergo considerable corrosion [2]. Significant reduction in corrosion rates has been achieved by various means including reduction of the metal impurity content, application of several surface modification techniques, thermal mechanical treatments as well as incorporation of suitable alloying elements. However, the use of corrosion inhibitors is the most practical and economical methods for corrosion protection and prevention of unexpected metal dissolution in aggressive acid media [3].

A number of hereto cyclic compounds have been reported as corrosion inhibitors for mild steel in HCl and screening of synthetic heterocyclic compounds is still being continued. All these studies reveal that heterocyclic compounds show significant inhibition efficiency due to the presence of hetero atoms such as N, O and S [4, 5]. The polar functional groups can absorb on the metal surface and block the active sites on the surface, thereby reducing the corrosion rate [6]. The

adsorption of organic molecules at the metal/solution interface plays an important role in surface science and can markedly improve the corrosion-resisting properties of metals [7].

Hydrazides constitute an important class of biologically active organic compounds and their therapeutic uses. Hydrazides and their condensation products are reported to possess a wide range of biological activities including antibacterial activity, tuberculostatic properties, antifungal and many more [8, 9]. Some aromatic hydrazides and its derivatives have been reported as efficient corrosion inhibitors for mild steel [10, 11]. Keeping in view the importance of hydrazide and its derivatives as potential corrosion inhibitors, 4-hydroxy-*N'*-[(1*E*, 2*E*)-3-phenylprop-2-en-1-ylidene] benzohydrazide (HPB) have been synthesized. The results of its corrosion inhibition action on mild steel in 0.5 M HCl are reported in this paper.

2. EXPERIMENTAL

2.1. Material

Commercially available grade of mild steel with composition of (% wt) C (0.159), Si (0.157), Mn (0.496), P (0.060), S (0.062), Cr (0.047), Ni (0.06), Mo (0.029), Al (0.0043), Cu (0.116) and rest iron was employed in this study. The specimen was prepared in the form of a cylindrical rod embedded in epoxy resin, having one end of the rod with an open surface area of 0.95 cm². Prior to the tests, the specimens were pol-

¹ The article is published in the original.

ished with different grades of emery polishing papers, respectively and finally on disc polisher using levigated alumina abrasive. The polished specimen was washed with double distilled water, cleaned with acetone, and finally dried before immersing in the medium

2.2. Medium

Stock solution of 0.5 M hydrochloric acid was prepared by diluting AR grade hydrochloric acid with double distilled water and was standardized by potentiometric method.

2.3. Inhibitor Preparation

HPB was prepared as per the reported literature [12]. An equimolar mixture of ethanolic solution of *trans*-3-Phenyl-2-propenal (0.01 mol) and 4-hydroxyl benzohydrazide (0.01 mol) was refluxed on a hot water bath for about 2h. The precipitated product was filtered, dried and recrystallized from ethanol. FTIR spectra of the dried sample was recorded using spectrophotometer (Schimadzu FTIR 8400S) in the frequency range of 4000 to 400 cm^{-1} using KBr pellets. The chemical structure of the HPB molecule is given in Fig. 1.

2.4. Electrochemical Measurements

Tafel polarization and electrochemical impedance spectroscopy were performed using a Potentiostat (CH Instrument USA Model 604D series with beta software). The measurements were carried out using a conventional three electrode Pyrex glass cell with platinum foil as the counter electrode and a saturated calomel electrode as the reference electrode. The mild steel specimen was used as the working electrode. Electrochemical impedance spectroscopy (EIS), measurements were carried out on the steady open circuit potential (OCP) disturbed with amplitude of 10 mV a.c. signal at the frequency range from 100 KHz to 10 mHz. Impedance data were analysed using Nyquist plots. The charge transfer resistance, R_{ct} was extracted from the diameter of the semicircle in the Nyquist plot. In Tafel polarization measurement, a finely polished mild steel specimen was exposed to 0.5 M HCl without and with inhibitor at different temperatures (30–60°C), and allowed to establish a steady state open circuit potential. The potentiodynamic polarization studies were then carried out in the potential range of –250 mV to +250 mV at a scan rate of 0.1 mV/s with respect to OCP.

2.5. Scanning Electron Microscopy (SEM)

The surface morphology of the mild steel specimen immersed in 0.5 M hydrochloric acid solution in the presence and absence of HPB were compared by recording the electron micrographs of the specimen

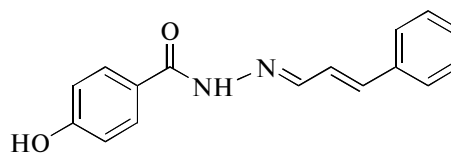


Fig. 1. Chemical structure of HPB.

using scanning electron microscope of model (EVO 18–5–57 model).

3. RESULTS AND DISCUSSION

3.1. Characterization of HPB

Crystalline white solid (95%); m.p: 264–266°C, $\text{C}_{16}\text{H}_{14}\text{N}_2\text{O}_2$. IR (KBr) [cm^{-1}]: 1612 (C=N str.), 1758 (C=O), 1558 (Ar. C=C str.), 3016 (CH str.), 3201 (NH str.), 2669 (C–H assy str), (2846 C–H sym str), 3502 (OH).

3.2. Electrochemical Impedance Spectroscopy

Electrochemical impedance spectroscopy is powerful technique to obtain information about the kinetics of interfacial mass transfer processes for mild steel corrosion in the presence of the studied inhibitor. Impedance measurements were undertaken in 0.5 M HCl without and with HPB in the range 0.1 mM to 0.8 mM and at the temperature range 30–60°C. The recorded electrochemical impedance spectroscopy spectra in inhibited and uninhibited solutions are presented in term of Nyquist plot as shown in Fig. 2.

The Nyquist plots showed one depressed capacitive loop, a single time constant for the impedance response. The observed depression of the capacitive loop, however, indicates frequency dispersion of interfacial impedance. This anomalous phenomenon is attributed to the nonhomogeneity of the electrode surface arising from the surface roughness or interfacial phenomena [13]. When such non-ideal frequency response is present, the capacitor is replaced by a constant phase element (CPE), with impedance Z_{CPE} as follows,

$$Z = Q^{-1}(i\omega)^{-n}, \quad (1)$$

Where Q is the proportionality coefficient, ω is the angular frequency, i is the imaginary number and n is the exponent related to the phase shift. If the value of $n = 1$, the CPE behaves like an ideal double layer capacitor [14].

The double layer capacitance is calculated using the following equation:

$$C_{dl} = \frac{1}{2\pi f_{max} R_{ct}}, \quad (2)$$

where, f_{max} is the frequency at which the imaginary component of impedance is maximum [15].

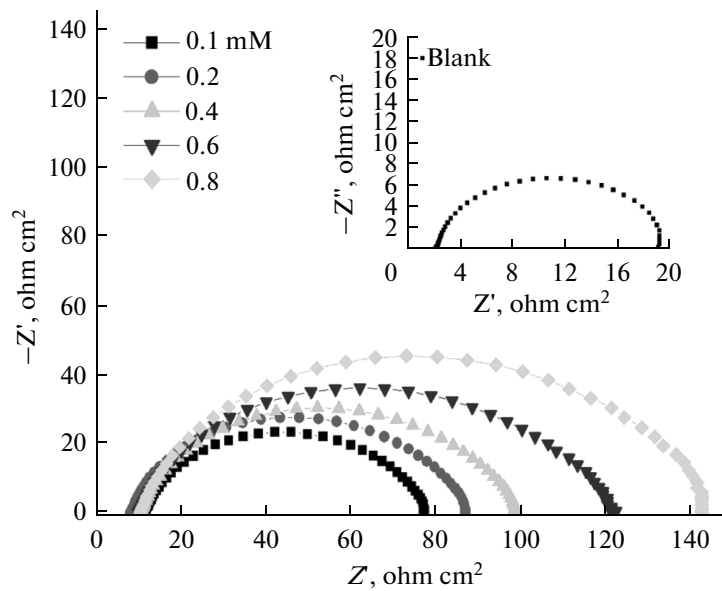


Fig. 2. Nyquist plots for corrosion of mild steel specimen in 0.5 M HCl containing different concentrations of HPB at 30°C.

The impedance spectra for the Nyquist plots were analysed by fitting into the equivalent circuit model, which has been used previously to model the iron/acid interface is shown in Fig. 3 [16]. In this equivalent circuit, R_s is the solution resistance, R_{ct} is the charge transfer resistance and CPE is a constant phase element. The resultant parameters were recorded in Table 1.

The values of IE (%) obtained from the charge-transfer resistances were calculated using the following equation:

$$\%IE = \frac{R_{ct} - R_{ct}^0}{R_{ct}} \times 100. \quad (3)$$

From the Table 1 it is clear that R_{ct} value increases with increase in concentration of HPB, and this in turn leads to an increase in IE (%). The increase in R_{ct} values is attributed to the formation of protective film on the metal/solution interface, which prevents the

charge transfer process [17]. Further the capacitance of the interface (C_{dl}) starts decreasing, with increase in inhibitor concentration, which is most probably due to the decrease in local dielectric constant and/or increase in thickness of the electrical double layer. This suggests that the inhibitor acts via adsorption at the metal/solution interface [18]. Thus, the decrease in C_{dl} values and the increase in R_{ct} values may be due to the gradual replacement of water molecules by the adsorption of the HPB molecules on the metal surface. This results in increasing the inhibition efficiency, which in turns decreases the extent of dissolution reaction [19].

3.3. Tafel Polarization Studies

The corrosion inhibition of mild steel in 0.5 M HCl containing various concentrations of HPB was studied using Tafel polarization technique and also the effect of temperature on the inhibition efficiency was studied using the same technique. Figure 4 represents Tafel polarization curves of the specimen in 0.5 M HCl containing different concentrations of HPB at 30°C.

The percentage inhibition efficiency ($\%IE$) is calculated from expression (4):

$$\%IE = \frac{i_{corr} - i_{corr(inh)}}{i_{corr}}, \quad (4)$$

where i_{corr} and $i_{corr(inh)}$ are the corrosion current densities in the absence and in the presence of inhibitor, respectively. The corrosion rate (CR) is calculated using following equation.

$$CR(\text{mm y}^{-1}) = \frac{3270 M i_{corr}}{qZ}, \quad (5)$$

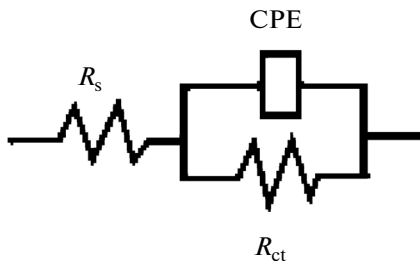


Fig. 3. Equivalent circuit used to fit experimental EIS data for the corrosion of mild steel in the absence and presence of HPB.

where 3270 is a constant that defines the unit of corrosion rate, i_{corr} = corrosion current density in A cm^{-2} , q = density of the corroding material, 7.75 g cm^{-3} , M = Atomic mass of the metal, and Z = Number of electrons transferred per metal atom [20] and the resultant parameters are tabulated in Table 2.

From the Table 2 it can be concluded that, the addition of HPB causes the resultant decrease in corrosion current density and corrosion rate of mild steel in 0.5 M HCl. Further the inhibition efficiency increases with increase in HPB concentration. The increase in % IE with increase in inhibitor concentrations is due to the blocking effect of the metal surface by both adsorption and film formation [21]. There is no change in the cathodic slope with increase in HPB concentration as well as with increase in temperature. This indicates that the hydrogen evolution is activation-controlled. The slight change in the anodic slope with HPB concentration at different temperatures indicates the influence of inhibitor on the kinetics of anodic reaction, but not on the mechanism [22]. Further there is no shift in E_{corr} values with increase in HPB concentration with respect to the blank. According to Ferreira et al [23], if the displacement in corrosion potential is more than $\pm 85 \text{ mV}$ with respect to corrosion potential of the blank, then the inhibitor can be considered as a cathodic or anodic type. This suggests that HPB acts as mixed type of inhibitor.

3.4. Effect of Temperature

The temperature as an environmental factor influencing the corrosion behaviour of mild steel in the absence and presence of HPB was studied by measuring the corrosion rate at different temperatures in the range 30–60°C. It can be observed that (Table 2) corrosion rate (CR) increase with increase in temperatures in the absence of inhibitor. This has been attributed to the reduction in hydrogen evolution over potential with the increase in temperature [21]. The addition of HPB brings down the corrosion rate to the minimal level. The inhibition efficiency of HPB increases with increase in temperature in 0.5 M HCl. The high protection efficiency of HPB at higher temperature is mainly due to its bonding interaction with the metal surface. The strong bonding is generally attributed to higher electron densities at active functional groups, imine group and π electrons present in the adsorbate molecules [24]. The small deviation in the b_c and b_a values with varying temperature, indicate that temperature play an influential role in the kinetics of the corrosion reactions. However in the presence of inhibitor the basic shape of polarization curves and Nyquist plots remain unaltered at all the temperature, which illustrates that temperature influences only the rate of corrosion but not the mechanism [22].

These results facilitate the evaluation of kinetic and thermodynamic parameters for the inhibition and interpretation of the mode of adsorption on the metal

Table 1. Impedance results for the corrosion of mild steel in 0.5 M HCl in the absence and presence of HPB at different temperatures

Temp (°C)	Conc. of HPB, mM	R_{ct} , $\Omega \text{ cm}^2$	C_{dl} , μF	% IE
30	0	16.75	1279	–
	0.1	86.34	77.58	80.5
	0.2	98.95	57.33	83.0
	0.4	108.21	47.82	84.5
	0.6	121.30	36.04	86.1
	0.8	135.0	25.81	87.6
40	0	10.01	2945	–
	0.1	53.76	151.1	81.3
	0.2	61.37	129.6	83.7
	0.4	66.71	116.3	85.0
	0.6	74.41	101.0	86.6
	0.8	85.44	82.97	88.2
50	0	5.70	10615	–
	0.1	34.79	354.8	83.6
	0.2	37.12	311.7	84.6
	0.4	45.0	235.7	87.3
	0.6	47.55	189.0	88.0
	0.8	51.75	172.3	89.0
60	0	2.33	45560	–
	0.1	16.32	1206	85.9
	0.2	19.46	938.0	88.1
	0.4	23.79	749.2	90.3
	0.6	27.87	581.1	91.7
	0.8	29.98	507.2	92.3

surface by the inhibitor. Energy of activation (E_a) for the corrosion of mild steel in 0.5 M HCl was calculated using the following equation [25]

$$\ln(CR) = B - \frac{E_a}{RT} \quad (6)$$

Where B is the Arrhenius pre-exponential constant, and R is the universal gas constant. Arrhenius plot ($\ln CR$ vs $1/T$) for the corrosion of mild steel in 0.5 M HCl is plotted as shown in Fig. 5. The slope ($-E_a/R$) obtained from the plot of $\ln(CR)$ against $1/T$ was used to calculate the activation energy for the corrosion process in the absence and presence of inhibitor.

The enthalpy of activation (ΔH^*) and entropy of activation (ΔS^*) for the metal dissolution process in the absence and presence of inhibitor are determined using the transition state equation [26].

$$CR = \frac{RT}{Nh} \exp\left(\frac{\Delta S^*}{R}\right) \exp\left(-\frac{\Delta H^*}{RT}\right), \quad (7)$$

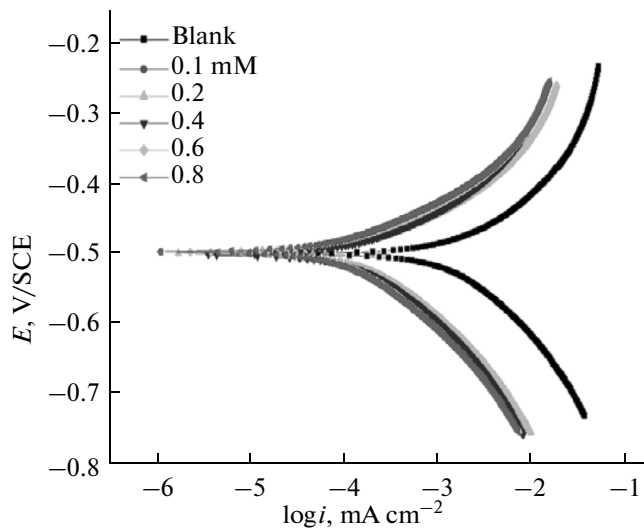


Fig. 4. Tafel polarization curves for the corrosion of mild steel specimen in 0.5 M HCl with various concentrations of HPB at 30°C.

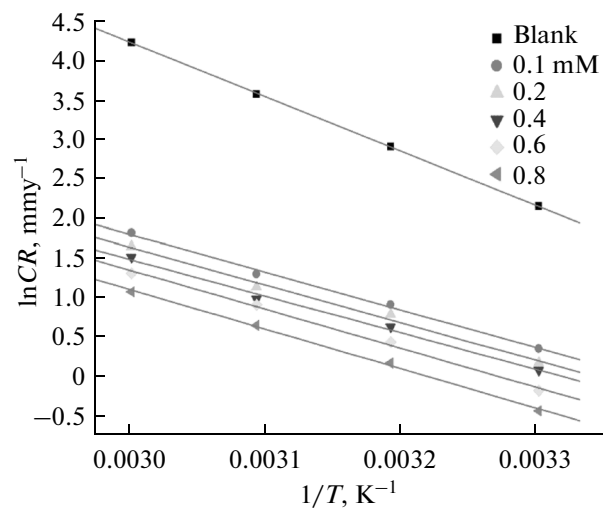


Fig. 5. Arrhenius plots for the corrosion mild steel in 0.5 M HCl with different concentrations of HPB.

Where h is Planck's constant and N is Avagadro's number. Fig. 6 shows the plot of $\ln (CR/T)$ vs $1/T$, gives a straight line with slope = $-\Delta H^*/T$ and intercept = $\ln(R/Nh) + \Delta S^*/R$. The activation parameters obtained in different concentration of HCl are recorded in Table 3.

It is found that the activation energy is lower in the presence of inhibitor than in its absence. This is due to the shift in the net corrosion reaction from that on the uncovered part of the metal surface to the covered one [27]. It is also observed that the whole process is controlled by surface reaction, since the activation energies of the corrosion process are above 20 kJ mol^{-1} [28]. The adsorption of the inhibitor on the electrode surface leads to the formation of a barrier layer between the metal surface and the corrosion medium, blocking the charge transfer, and thereby reducing the metal reactivity in the electrochemical reactions of corrosion.

The ΔS^\ddagger is negative; implying the activated complex in the rate-determining step represents association rather than dissociation, indicating that a decrease in randomness takes place on going from the reactants to the activated complex [29].

3.5. Adsorption Isotherm

Generally the adsorption isotherm provides useful insights into the characteristics of the adsorption process and the mechanism of corrosion inhibition. The degree of surface coverage (θ) at different concentrations of the inhibitor is evaluated from potentiodynamic polarization measurements. The data were tested graphically by fitting to various isotherms. The Langmuir adsorption isotherm was found to fit well with the experimental data, as shown in Fig. 7, and can be expressed as,

$$\frac{C_{inh}}{\theta} = \frac{1}{K_{ads}} + C_{inh}, \quad (8)$$

Where, C_{inh} is the inhibitor concentration, and K_{ads} the adsorptive equilibrium constant, and θ representing the degree of adsorption [30].

The slopes of the isotherms show deviation from the value of unity as would be expected for the ideal Langmuir adsorption isotherm equation. This deviation from unity may be due to the interaction among the adsorbed species on the metal surface. The polar groups or hetero atoms present in the case of inhibitor molecules are adsorbed at the anodic or cathodic sites of the metal surface. These adsorbed species may interact by mutual attraction or repulsion [31]. Thus,

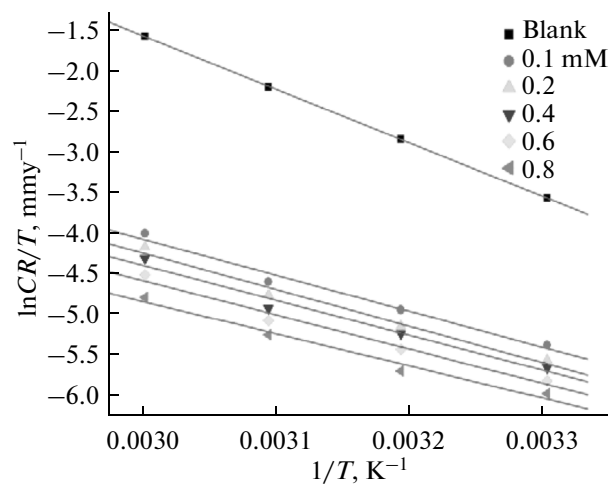


Fig. 6. Plot of $\ln (CR)/T$ versus $1/T$ for corrosion of mild steel specimen in 0.5 M HCl containing various concentrations of HPB.

Table 2. Tafel polarization results for the corrosion of mild steel in 0.5 M HCl in the absence and presence of inhibitor at various temperatures

Temp, °C	Conc. of HPB, mM	E_{corr} , mV/SCE	$-b_c$, mV dec ⁻¹	b_a , mV dec ⁻¹	i_{corr} , mA cm ⁻²	CR, mmy ⁻¹	% IE
30	0	-480	84.21	86.06	1.4050	8.71	—
	0.1	-508	79.07	90.66	0.2292	1.43	83.6
	0.2	-506	86.22	106.45	0.1920	1.19	86.3
	0.4	-505	84.87	103.78	0.1748	1.08	87.5
	0.6	-502	87.52	106.87	0.1219	0.76	91.3
	0.8	-501	89.09	113.35	0.1041	0.65	92.7
40	0	-474	69.89	68.76	3.0010	18.60	—
	0.1	-508	82.88	96.82	0.4048	2.52	86.5
	0.2	-507	82.63	98.99	0.3575	2.22	88.0
	0.4	-507	79.42	96.26	0.3036	1.88	89.9
	0.6	-508	79.56	93.54	0.2775	1.72	90.7
	0.8	-507	81.60	96.13	0.2098	1.31	93.0
50	0	-476	61.38	57.32	5.8870	36.50	—
	0.1	-509	78.52	89.80	0.5375	3.33	90.8
	0.2	-509	79.73	92.64	0.4557	2.82	92.2
	0.4	-507	78.68	94.52	0.3874	2.40	93.4
	0.6	-507	77.39	93.13	0.3689	2.29	93.7
	0.8	-507	78.89	92.88	0.3423	2.12	94.1
60	0	-476	54.84	52.38	11.350	70.38	—
	0.1	-511	74.63	81.88	1.005	6.23	91.1
	0.2	-513	72.93	89.25	0.8469	5.25	92.5
	0.4	-513	70.63	88.30	0.7381	4.57	93.4
	0.6	-518	74.63	81.41	0.6650	4.12	94.1
	0.8	-512	78.35	77.99	0.4618	2.83	95.9

the inhibiting effect of HPB molecules on the mild surface in 0.5 M HCl solution slightly deviates from ideal Langmuir adsorption isotherm.

The values of standard free energy of adsorption ΔG_{ads}° , are related to K_{ads} by the relation. The calculated values of ΔG_{ads}° , are tabulated in Table 4.

$$K = \frac{1}{55.5} \exp\left(\frac{-\Delta G_{ads}^\circ}{RT}\right), \quad (9)$$

Where R is the universal gas constant, T is the absolute temperature, and 55.5 is the concentration of water in solution in mol dm⁻³[32].

The plot of ΔG_{ads}° versus T showed straight line is shown in Fig. 8.

The standard enthalpy of adsorption (ΔH_{ads}°) and the standard entropy of adsorption (ΔS_{ads}°) are computed from the slope and intercept of the straight line respectively according to the thermodynamic equa-

tion (10) and, the resulting values of thermodynamic parameters are recorded in Table 4.

$$\Delta G_{ads}^\circ = \Delta H_{ads}^\circ - T\Delta S_{ads}^\circ, \quad (10)$$

Table 3. Activation parameters for the corrosion of mild steel in 0.5 M HCl containing different concentrations of HPB

Conc. of HPB, mM	E_a , kJmol ⁻¹	ΔH^\ddagger , kJmol ⁻¹	ΔH^\ddagger , Jmol ⁻¹ K ⁻¹
0	57.76	55.12	44.95
0.1	39.99	37.67	119.82
0.2	39.98	37.10	119.82
0.4	38.87	36.00	125.80
0.6	38/09	35.26	129.59
0.8	37.02	33.10	138.21

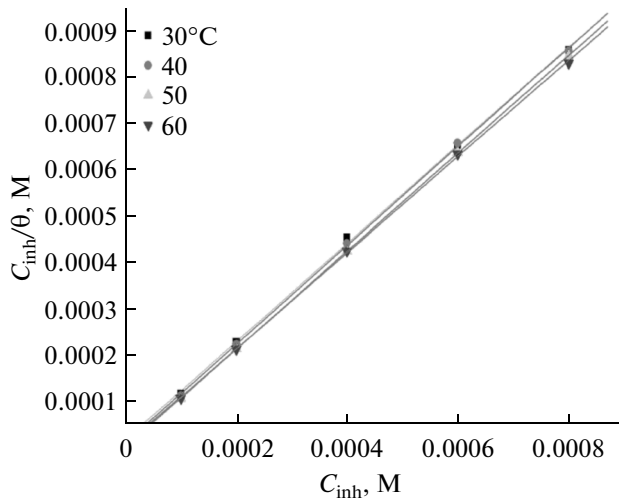


Fig. 7. Langmuir's adsorption isotherm of HPB on corrosion of mild steel in 0.5 M HCl at different temperatures.

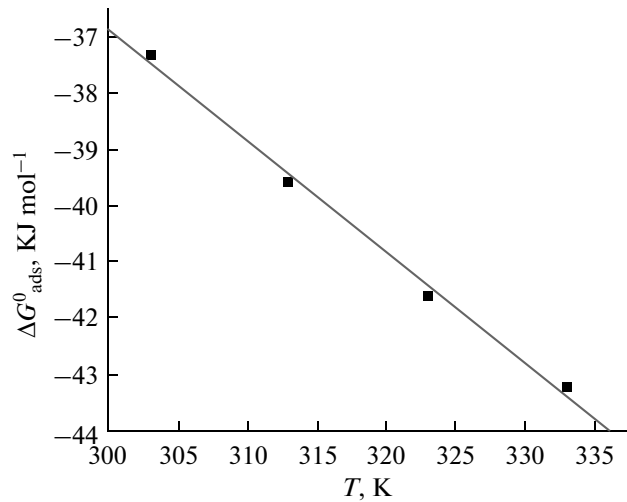


Fig. 8. Plot of ΔG_{ads}° versus T for the adsorption of HPB on mild steel in 0.5 M HCl.

From Table 5, the negative ΔG_{ads}° values indicate the spontaneity of the adsorption process and stability of the adsorbed layer on the metal surface. Generally, the values of ΔG_{ads}° lower than -20 kJ mol^{-1} are consistent with physisorption, while those around -40 kJ mol^{-1} or higher correspond to chemisorptions [33]. In the present study the calculated the ΔG_{ads}° values found to be very close to 40 kJ mol^{-1} particularly at lower temperature and increases with increase in temperature. This indicates the studied inhibitor getting physical adsorbed on the metal surface at lower temperature and predominantly chemisorption favours as the temperature increases [34]. The positive value of enthalpy of adsorption indicates that the adsorption of the inhibitor molecule is an endothermic process. Generally, an exothermic adsorption process signifies either physical adsorption or chemical adsorption, while the endothermic process is attributable unequivocally to chemical adsorption [35]. In the present investigation positive value of enthalpy of adsorption proves that adsorption of the inhibitor is by a chemical

adsorption process. ΔS_{ads}° values in the presence of the inhibitor are negative, indicating that an increase in orderliness takes place on going from the free state to the adsorbed state of the inhibitors. This might be attributed to the orderly adsorption of the inhibitor molecules from a chaotic state of the freely moving molecules in the solution [36].

3.7. Inhibition Mechanism

The results obtained from the Tafel polarization and EIS technique, it is concluded that the HPB inhibit the corrosion of mild steel in 0.5 M HCl by adsorption at metal solution interface. It is general assumption that the adsorption of organic inhibitors at the metal solution interface is the first step in the mechanism of the inhibitor action [37]. Organic inhibitor molecule may adsorb on the metal surface in the following ways, namely:

- i—Electrostatic interaction between the charged inhibitor molecules and the charged metal,
- ii—Interaction of unshared electron pairs in the inhibitor molecule with the metal,

Table 4. Thermodynamic parameters for the adsorption of HPB on mild steel surface in 0.5 M HCl acid at various temperatures

Temp, °C	K_{ads}, M^{-1}	Slope	$-\Delta G_{ads}^{\circ}, \text{kJ mol}^{-1}$	$-\Delta H_{ads}^{\circ}, \text{kJ mol}^{-1}$	$-\Delta S_{ads}^{\circ}, \text{J mol}^{-1} \text{K}^{-1}$
30	49139.8	1.060	37.33	22.08	196.6
40	73204.9	1.067	39.59		
50	111006.2	1.057	41.98		
60	108738.0	1.038	43.22		

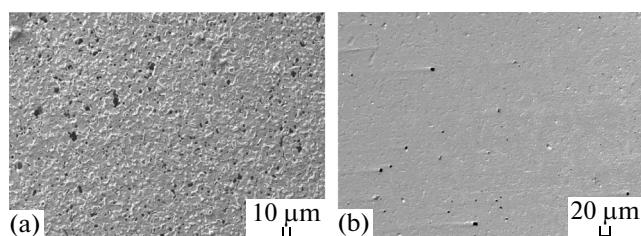
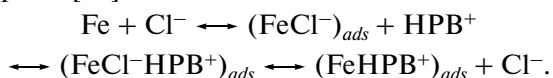


Fig. 9. SEM images of the mild steel a) Exposed to 0.5 M HCl solution and (b) Exposed to 0.5 M HCl containing 0.8 mM of HPB.

iii—Interaction of π -electrons of the inhibitor molecule with the metal and

iv—The combination of two or more of the above steps.

In the present case HPB get protonated in HCl medium at nitrogen atoms of the hydrazide group, which results in the formation of positively charged inhibitor species, which will electrostatically interact with negative charge formed at the metal acid solution interface, thereby facilitating physisorption. In addition the protonated inhibitor molecules can also be adsorbed at cathodic sites of metal in competition with hydrogen ions. The adsorption of protonated HPB molecules reduces the rate of hydrogen evolution reaction along with metal oxidation resulting in physisorption [38].



Further the unprotonated or neutral molecule of HPB can also adsorb via chemisorption on the vacant sites on the mild steel surface either by sharing of electrons between the hetero atoms of HPB and metal surface or by the interaction of π electrons of the aromatic ring of the HPB molecule with that of mild steel surface. Since in mild steel iron contains vacant $3d$ orbital which can form coordinate type of bond with inhibitor due to interaction of electron rich π -electron clouds of aromatic rings as well as unshared electron pairs on nitrogen or oxygen atoms of the HPB leading to predominantly chemisorption [39].

3.8. Scanning Electron Microscopy

SEM investigations were carried out to differentiate between the surface morphology of the metal surface, immediately after its immersion in 0.5 M hydrochloric acid for three hours in the absence and presence of HPB. Figure 9a, 9b shows the surface images of mild steel sample in the absence and presence of HPB respectively. The closed observation of Fig. 9a shows the formation of rough surface including pits due to the corrosion, whereas smooth sample surface was obtained in the presence of HPB as shown in Fig. 9b. This confirms the adsorption of HPB on the mild steel surface through the formation of protective film.

4. CONCLUSION

HPB acts as potential inhibitor for the corrosion control of mild steel in 0.5 M hydrochloric acid solution. The percentage inhibition efficiency increases with increase in HPB concentrations and with increase in the temperature. It showed maximum inhibition efficiency, more than 90% at its optimum concentration at all the studied temperature. Tafel polarization measurements indicate HPB acts as mixed type inhibitor. The adsorption of HPB on the mild steel surface obeys Langmuir adsorption isotherm and adsorption of HPB is through mixed type adsorption, with predominately chemisorption.

ACKNOWLEDGMENTS

The authors are grateful to Manipal University and chemistry department, Manipal Institute of Technology Manipal, for providing laboratory facility.

REFERENCES

- Vishwanatham, S. and Haldar, N., *Corros. Sci.*, 2008, vol. 50, p. 2999.
- Bothi, R.P. and Sethuraman, M.G., *Mater. Lett.*, 2008, vol. 62, p. 113.
- Satapathy, A.K., Gunasekaran, G., Sahoo, S.C., et al., *Corros. Sci.*, 2009, vol. 51, p. 2848.
- Emregal, C.K. and Mustafa, H., *Corros. Sci.*, 2006, vol. 48, p. 797.
- Khaled, K.F., Babic-Samradzija, K., and Hackerman, N., *Electrochim. Acta*, 2005, vol. 50, p. 2515.
- Roberge, P.R., *Corrosion Inhibitors: Handbook of Corrosion Engineering*, New York: McGraw-Hill, 1999.
- Quartarone, G., Battilana, M., Bonaldo, L., et al., *Corros. Sci.*, 2008, vol. 50, p. 3467.
- Haksar, C.N., Malhotra, R.C., Pandya, G., et al., *J. Sci. Technol. B*, 1971, vol. 9, p. 34.
- Kraatz, L.U., Wolfgang, B.K., Wolfram, B.G.A., et al. US Patent 5929118, 1999.
- Quraishi, M.A., Sardar, R., and Jamal, D., *Mater. Chem. Phys.*, 2001, vol. 71, p. 309.
- Shanbhag, A.V., Venkatesha, T.V., Prabhu, R., et al., *J. Appl. Electrochem.*, 2008, vol. 38, p. 279.
- Renata, B.O., Elaine, M.S.F., and Rodrigo, P.P.S., *Eur. J. of Med. Chem.*, 2008, vol. 43, p. 1984.
- Flis, J. and Zakroczymski, T., *J. Electrochem. Soc.*, 1996, vol. 143, p. 2458.
- Rammelt, U., Kohler, S., and Reinhard, G., *Electrochim. Acta*, 2008, vol. 53, p. 6968.
- Hsu, C.H. and Mansfeld, F., *Corrosion*, 2001, vol. 57, p. 747.
- Larabi, L., Benali, O., Mekelleche, S., et al., *Appl. Surf. Sci.*, 2006, vol. 253, p. 1371.
- McCafferty, E. and Hackerman, N., *J. Electrochem. Soc.*, 1972, vol. 119, p. 146.
- Muralidharan, S., Phani, K.L., Pitchumani, S., et al., *J. Electrochem. Soc.*, 1995, vol. 142, p. 1478.

19. Fontana, M.G., *Corrosion Engineering*, Singapore: McGraw-Hill, 1987, 3rd ed.
20. Rafique, M.Z.A., Saxena, N., Khan, S., et al., *Indian J. Chem. Technol.*, 2007, vol. 14 576.
21. Wang, L., Shinohara, T., Zhang, B., et al., *J. Alloys Compd.*, 2010, vol. 496, p. 500.
22. Ferreira, E.S., Giancomelli, C., Giacomelli, F.C., et al., *Mater. Chem. Phys.*, 2004, vol. 83, p. 129.
23. Shrier, L.L., Jarman, R.A., and Burstein, G.T. *Corrosion*, Oxford, UK: Butterworth-Heinemann, 2000, 3rd ed.
24. Yahalom, J., *Corros. Sci.*, 1972, vol. 12, p. 867.
25. Abd Ei-Rehim, S.S., Ibrahim, M.A., and Khaled, K.F., *J. Appl. Electrochem.*, 1999, vol. 29, p. 595.
26. Schmid, G.M. and Huang, H.J., *Corros. Sci.*, 1980, vol. 20, p. 1041.
27. Li, W., He, Q., Zhang, S., et al., *J. Appl. Electrochem.*, 2008, vol. 38, p. 289.
28. Ishwara Bhat, J. and Alva, V.D.P., *Trans. Indian Inst. Met.*, 2011, vol. 64, p. 377.
29. Ashassi-Sorkhabi, H., Majidi, M.R., and Seyyed, K., *Appl. Surf. Sci.*, 2004, vol. 225, p. 176.
30. Badr, G.E., *Corros. Sci.*, 2009, vol. 51, p. 2529.
31. Paul, V. and Kar, B., *ISRN Corros.*, 2012, vol. 2012.
32. Fekry, A.M. and Ameer, M.A., *Int. J. Hydrogen Energy*, 2010, vol. 35, p. 7641.
33. Singh, A.K. and Quraishi, M.A., *Corros. Sci.*, 2011, vol. 53, p. 1288.
34. Oguzie, E.E.N., Joku, V.O., Enenebeaku, C.K., et al., *Corros. Sci.*, 2008, vol. 50, p. 3480.
35. Durnie, W., Marco, R.D., Jefferson, A., et al., *J. Electrochem. Soc.*, 1999, vol. 146, p. 17.
36. Martinez, S. and Stern, I., *Appl. Surf. Sci.*, 2002, vol. 199, p. 83.
37. Bockris, J.O.M., Devanathan, M.A., and Mulle, K., *Proc. R. Soc. A*, 1963, vol. 274, p. 55.
38. Khaled, K.F. and Hackerman, N., *Electrochem. Acta*, 2003, vol. 48, p. 2715.
39. Popova, A., Sokolova, E., Raicheva, S., et al., *Corros. Sci.*, 2003, vol. 45, p. 33.